

HIGH RESOLUTION REMOTE SENSING MISSIONS  
OF A TETHERED SATELLITE

S. Vetrella - A. Moccia

Chair of Aerospace Systems Engineering  
Institute of Gasdynamics, University of Naples  
p.le Tecchio 80, I-80125 Naples Italy

Abstract

This paper deals with the application of the Tethered Satellite (TS) as an operational remote sensing platform. It represents a new platform capable of covering the altitudes between airplanes and free flying satellites, offering an adequate lifetime, high geometric and radiometric resolution and improved cartographic accuracy.

Two operational remote sensing missions are proposed: one using two linear array systems for along-track stereoscopic observation and one using a synthetic aperture radar combined with an interferometric technique. These missions are able to improve significantly the accuracy of future real time cartographic systems from space, also allowing, in the case of active microwave systems, the Earth's observation both in adverse weather and at any time, day or night.

Furthermore a simulation program is described in which, in order to examine carefully the potentiality of the TS as a new remote sensing platform, the orbital and attitude dynamics description of the TSS is integrated with the sensor viewing geometry, the Earth's ellipsoid, the atmospheric effects, the sun illumination and the digital elevation model.

In order to test and check this model and to focus the attention of remote sensing users and researchers, a preliminary experiment has been proposed which consists of a metric camera to be deployed downwards during the second Shuttle demonstration flight.

This paper has been realized with the financial support of the Space Plan of the Italian National Research Council (CNR/PSN contract no. 84/049).

PRECEDING PAGE BLANK NOT FILMED

## Introduction

In the last few years several experiments of remote sensing have been conducted using free flying satellites at different altitudes. The results have shown the need for an increasing performance of future advanced multispectral imaging systems.

First, it is likely that significant improvement in sensor resolution will be required. Secondly, it may be desirable to use significantly narrower spectral bandwidths. In addition, many remote sensing disciplines have stated a need for high sensitivities capable of detecting a few tenths of a percent change in reflectivity for background reflectivities in the order of 5%. Lastly, increasing resolution must be combined with stereoscopic coverage particularly for completion and revision of world's cartography.

Based on these considerations, new sensor technologies have been developed and new space missions have been approved such as the French SPOT satellite, the U.S. LANDSAT D and Large Format Camera and the German MOMS and RMK etc. The Space Shuttle now gives the unique capability of a low orbit in which different remote sensing systems can be tested, before their operational life.

In spite of these actual and future improvements, there are practical limitations in the achievable geometric and radiometric resolutions and in the height measurement accuracy from space.

The unique capability of the Tethered Satellite System (TSS) to deliver payloads to altitudes down to 120 Km and to make relevant measurements on a global scale allows the observation of the Earth and the atmosphere with sensors of simplified design and/or of better performance with respect to those of platforms at higher altitudes. This is particularly true when high geometric resolution and S/N ratio are required using different narrow spectral bands. The Tethered Satellite (TS) deployed by the Shuttle or by a future space station is candidate as an operational platform capable of covering the altitudes between airplanes and free flying satellites. Furthermore it offers unique advantages in improving the results obtainable by push-brooms and passive and active microwave sensors.

The first part of this paper deals with a preliminary analysis of the different advantages and problems of two potential remote sensing missions, which allow the stereoscopic observation of the Earth by using two solid state sensors or a Synthetic Aperture Radar (SAR), onboard the TS.

The second part gives a synthetic description of the computer simulation program developed by the authors (in which the TS orbital and attitude dynamics is integrated with the sensor observation) and of the experiment proposed for the second Shuttle demonstration mission.

### Remote sensing missions of a multipurpose TS deployed by a Space Station

Most applications of a remote sensing require a repetitive coverage of large areas of the Earth and, consequently, need an adequate satellite lifetime. Therefore, even though the TS deployed by the Space Shuttle is a platform particularly suited for testing new sensors and for carrying out scientific experiments, its operational use as a high resolution remote sensing platform is strictly connected to the development of space stations. The flexibility offered by a recoverable multipurpose tethered platform, deployable at different altitudes and able to exploit all the advantages of being connected to the space station (power, data handling, human intervention, etc.) will permit several remote sensing experiments to be conducted such as:

- development of a modular multi-altitude sensor;
- integration of data at different resolution from different platforms;
- high geometric and radiometric resolution in the visible and infrared;
- development of active and passive microwave systems using tethered antennas;
- analysis of the bidirectional reflectance coefficient using a multiangle approach.

Taking into account the inadequacy of current topographic map coverage to meet worldwide needs for economic planning and development, the TS offers in particular new possibilities for creation and maintenance of cartographic information. Therefore, in the following, special emphasis is devoted to the operational application of the TS to topographic and thematic mapping, by giving two examples of stereoscopic observation using a linear array and a SAR interferometer system.

Photogrammetric cameras and frame sensors will not be considered due to the fact that their application and improved performance at lower altitudes are well known.

The along-track stereoscopic coverage using two linear arrays (fig. 1) requires particular constraints on the satellite position and attitude dynamics, which are analyzed in the following, in order to identify the achievable scale improvement using the TSS, under the assumption of a circular orbit and the same EIFOV, with respect to the deployer (DP) or a free flying (FF) satellite. The TS gives a small improvement of the integration time (T) and a small increase of the time interval between the fore and aft camera observations in comparison with a free-flying satellite at the same altitude (fig. 2). The dashed lines show the ratio of the integration time between the TS and the deployer. The sensor simplified design is mainly due to the reduced optics aperture and focal length (fig. 3).

The basic "heighting" equation for convergent linear array image stereopairs (fig. 1) is (ref. 1):

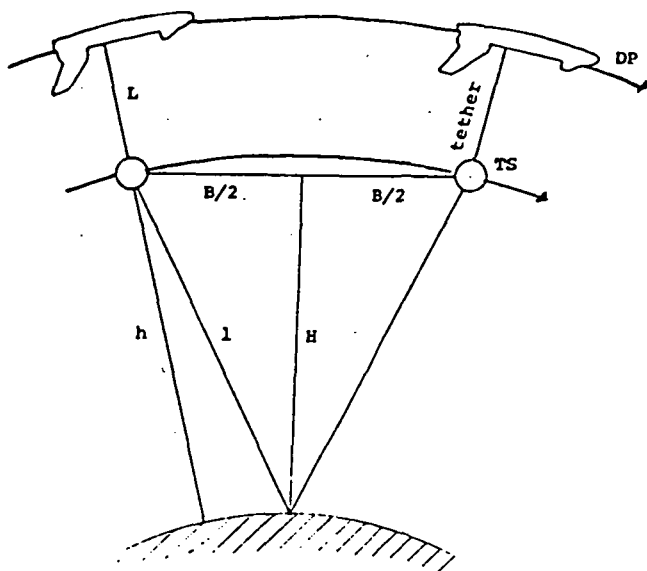


Fig. 1 Fore and aft camera stereoscopic viewing geometry from the tethered satellite.

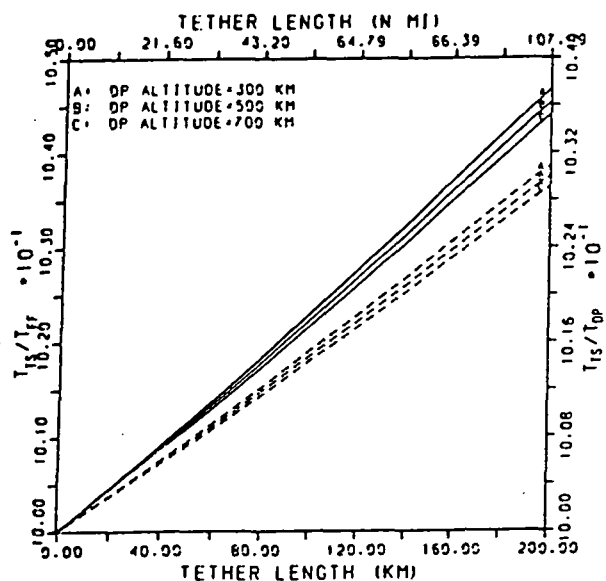


Fig. 2 Ratio between the integration times of the TS and of the FF satellite and of the DP (dashed lines) as function of tether length.

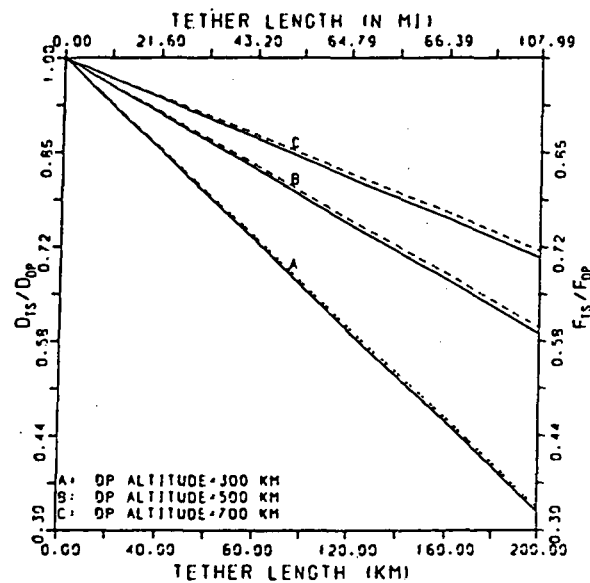


Fig. 3 Ratio between the optics aperture diameters and the focal lengths (dashed lines) of the TS and of the DP, as a function of tether length.

$$\Delta h = \frac{\Delta p}{(B/H)} SF$$

where  $\Delta h$  is the height difference,  $\Delta p$  is the difference in x-parallax, SF is the image scale factor, B/H is the base to height ratio.

The ratio between the spot height error (Z-error, ZE) of the TS and DP is shown in fig. 4, using two different values of the ratio  $(B/H)_{DP}/(B/H)_{TS}$ . This figure points out that the increased tether length, which reduces the sensor EIFOV and swath width, decreases the TS Z-error, under the same B/H ratio of the deployer or allows reduction of the TS B/H ratio under the same Z-error. The advantages of using the TS with respect to the deployer are made more evident by decreasing the DP altitude.

Under the same B/H ratio, the TS needs a time interval between the fore and aft cameras shorter than the interval of the deployer. This is important from the geometrical point of view, since any perturbation in the satellite attitude, altitude or velocity will be translated into geometric distortions in the imagery, giving rise to loss of planimetric and vertical cartographic accuracy (fig. 5). Under the same along-track angular error, at lower altitudes, it is possible to achieve a better Z-error (fig. 6).

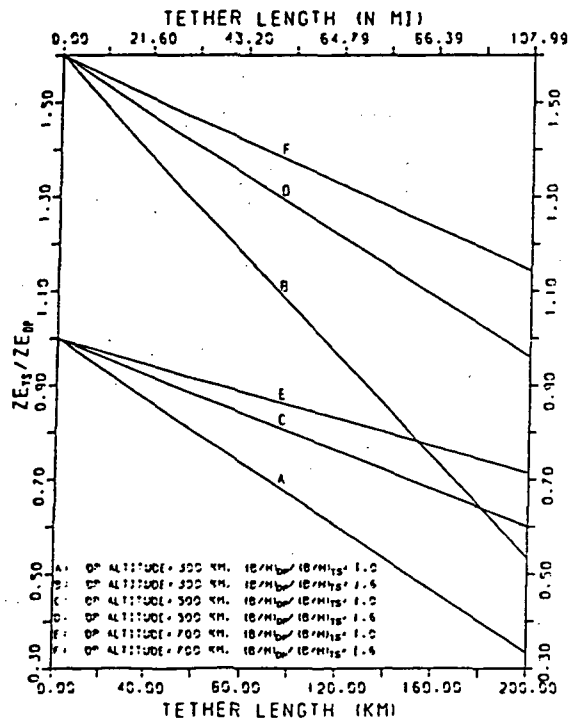


Fig. 4 Ratio between the spot height error of the TS and the DP as a function of tether length.

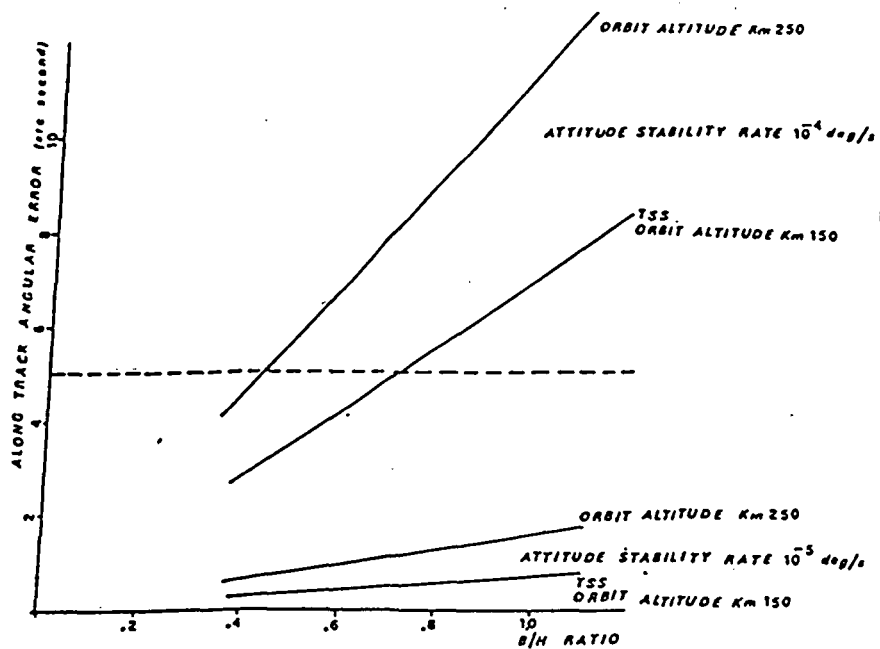


Fig. 5 Along-track angular error vs. B/H ratio for different attitude stability rates and orbit altitudes.

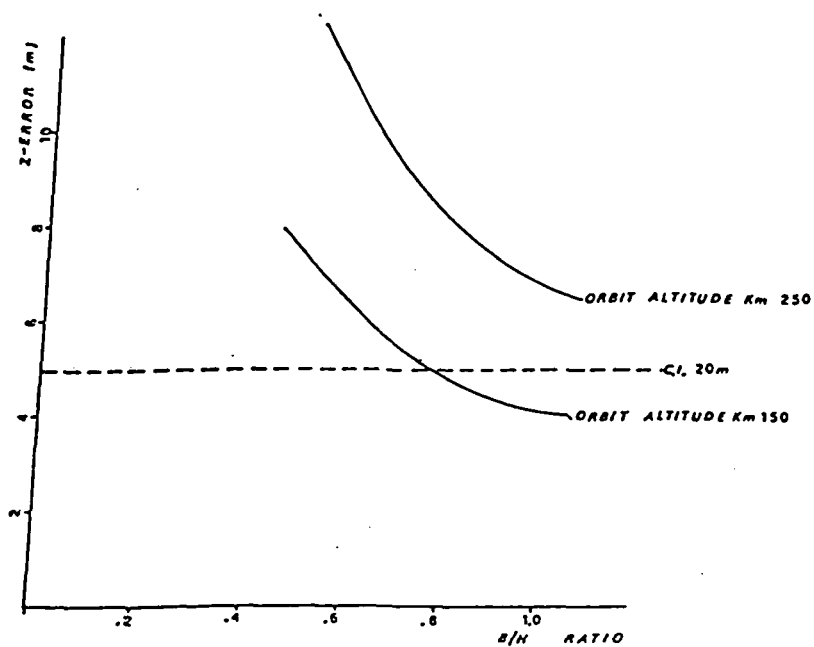


Fig. 6 Z-error vs. B/H ratio for different orbit altitudes. Dashed line shows the value for contour interval 20 m.

The along-track stereoscopic coverage involves the reduction of the swath width, due to the Earth's rotation between the fore and aft camera observations. A yaw motion has been proposed (ref. 2) to reduce the lack of coverage.

In the case of the TS, the decrease of  $\Delta t$  between two successive observations of the same point is partly balanced by the swath width reduction. This effect, at the ascending node, is shown by the following equations, in which the chord is assumed equal to the arc (fig. 1),  $K$  represents the ratio between the Earth's displacement and the swath width ( $W$ ), during the fore and aft camera observations,  $R_{\oplus}$  is the Earth's radius,  $\mu$  is the Earth's gravitational constant, and  $\omega_{\oplus}$  is the Earth's rotational rate:

$$K = \frac{\omega_{\oplus} R_{\oplus} \left( \frac{B}{H} \right) (H + L)}{W_{DP} \left\{ \frac{R_{\oplus} + H}{R_{\oplus} + H + L} \right\} \sqrt{\frac{\mu}{R_{\oplus} + H + L}}}$$

$$\frac{K_{TS}}{K_{DP}} = \frac{\left( \frac{B}{H} \right)_{TS}}{\left( \frac{B}{H} \right)_{DP}} \left( \frac{R_{\oplus} + H + L}{R_{\oplus} + H} \right)$$

In this case a substantial gain in the effective stereoscopic coverage can be obtained using the possibility of reducing the  $B/H$  ratio as a function of the tether length.

As previously shown a decrease of the  $B/H$  ratio improves the attitude stability  $Z$ -error and worsens the measurement  $Z$ -error.

The swath width is connected to the EIFOV and data rate as shown in figs. 7-8. The TS offers the possibility of decreasing the data rate (for a constant ratio Earth's displacement/swath width) and this effect is increased by decreasing the EIFOV.

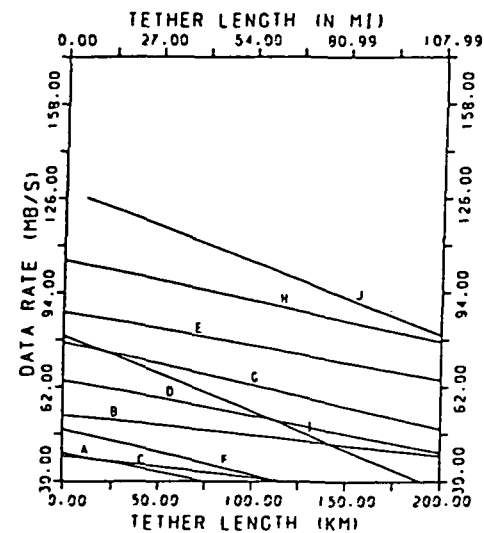
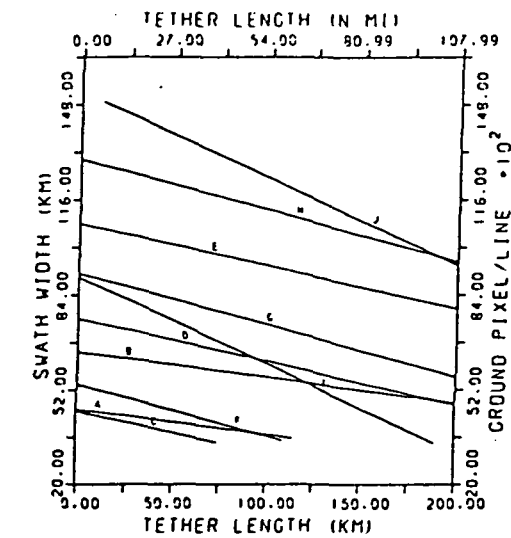
A representative example is given by a space station orbiting at an altitude of 500 Km, having, as an operational module, a TS that can be deployed to 200 Km. The following root mean square  $Z$ -errors must be taken into account to get an estimate of the final scale:

- measurement error (fig. 4), assumed equal to 1/2 pixel;
- error due to the attitude stability rate ( $10^{-5}$  °/s);
- miscellaneous errors, assumed less than 1 pixel.

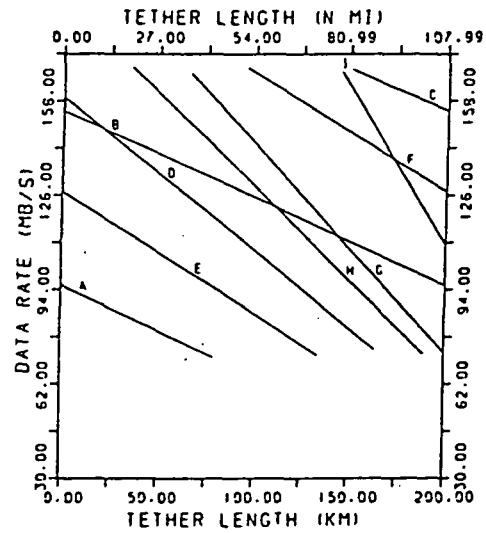
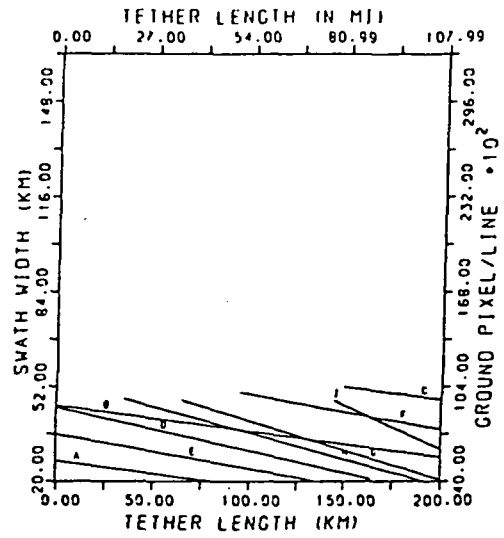
Table 1 illustrates also the scales that can be reached at different altitudes.

Another method that can be proposed for high resolution observation with contemporaneous terrain height measurement is the interferometric technique which consists of two antennas one above the other.

If two vertically spaced physical antennas are carried along parallel paths by the deployer and the TS, the outputs of the two synthetic antenna systems can be combined to form a synthe-



A: DP ALTITUDE=300 KM. B/H=0.6. DISPL./SWATH WIDTH=0.4  
 B: DP ALTITUDE=700 KM. B/H=0.6. DISPL./SWATH WIDTH=0.4  
 C: DP ALTITUDE=300 KM. B/H=1.0. DISPL./SWATH WIDTH=0.4  
 D: DP ALTITUDE=500 KM. B/H=1.0. DISPL./SWATH WIDTH=0.4  
 E: DP ALTITUDE=700 KM. B/H=1.0. DISPL./SWATH WIDTH=0.4  
 F: DP ALTITUDE=300 KM. B/H=0.6. DISPL./SWATH WIDTH=0.2  
 G: DP ALTITUDE=500 KM. B/H=0.6. DISPL./SWATH WIDTH=0.2  
 H: DP ALTITUDE=700 KM. B/H=0.6. DISPL./SWATH WIDTH=0.2  
 I: DP ALTITUDE=300 KM. B/H=1.0. DISPL./SWATH WIDTH=0.2  
 J: DP ALTITUDE=500 KM. B/H=1.0. DISPL./SWATH WIDTH=0.2  
 EIFOV=10 M



A: DP ALTITUDE=300 KM. B/H=0.6. DISPL./SWATH WIDTH=0.4  
 B: DP ALTITUDE=500 KM. B/H=0.6. DISPL./SWATH WIDTH=0.4  
 C: DP ALTITUDE=700 KM. B/H=0.6. DISPL./SWATH WIDTH=0.4  
 D: DP ALTITUDE=300 KM. B/H=1.0. DISPL./SWATH WIDTH=0.4  
 E: DP ALTITUDE=500 KM. B/H=1.0. DISPL./SWATH WIDTH=0.4  
 F: DP ALTITUDE=700 KM. B/H=1.0. DISPL./SWATH WIDTH=0.4  
 G: DP ALTITUDE=300 KM. B/H=0.6. DISPL./SWATH WIDTH=0.3  
 H: DP ALTITUDE=500 KM. B/H=0.6. DISPL./SWATH WIDTH=0.3  
 I: DP ALTITUDE=700 KM. B/H=0.6. DISPL./SWATH WIDTH=0.3  
 J: DP ALTITUDE=300 KM. B/H=1.0. DISPL./SWATH WIDTH=0.3  
 EIFOV=5 M

Fig. 7 Swath width and data rate as a function of tether length for different deployer altitudes, B/H ratios, Earth's displacement/swath width ratios and EIFOV = 10 m.

Fig. 8 Same as fig. 7 for EIFOV = 5 m.



NMAS SPOT HEIGHT ZE (m)	MAP SCALE	TS ALTITUDE (Km)	EIFOV (m)	ATTITUDE STABILITY ZE (m)	MEASUREMENT ZE (m)	MISCELLANEOUS ZE (m)	TOTAL ZE (m)
$\pm 6-15$	1:100,000	500	10	$\pm 7.0$	$\pm 5$	$\pm 8$	$\pm 11.7$
		400	8	$\pm 4.6$	$\pm 4$	$\pm 6$	$\pm 8.6$
$\pm 6$	1:50,000	300	6	$\pm 2.6$	$\pm 3$	$\pm 4$	$\pm 5.6$

Table 1 Achievable scales of topographic maps from different altitudes ( $B/H = 1$ , attitude stability rate  $10^{-5}$  °/s).

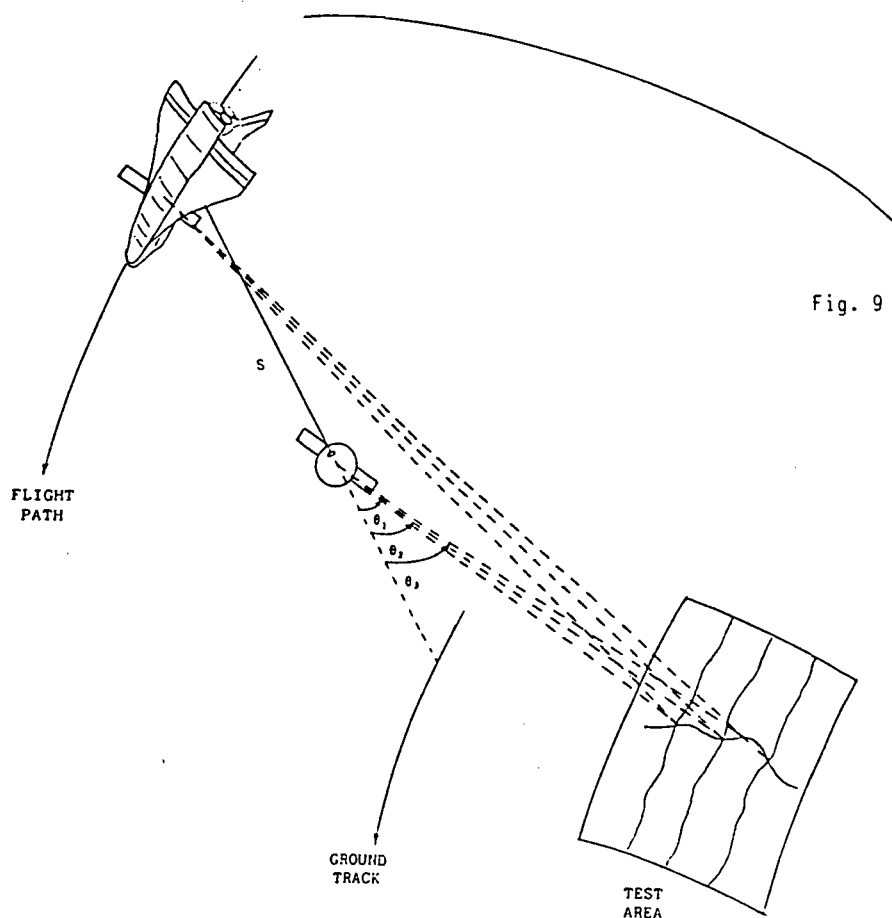


Fig. 9 SAR interferometer configuration.

tic interferometer (fig. 9). The fine resolution image of the terrain is provided by synthetic aperture radar technology (ref. 3) and the height measurement is made by radar interferometry (ref. 4). Therefore two images are produced: one using the normal synthetic aperture radar image obtainable by a single physical antenna, and one using two antennas to produce the null pattern that can be superimposed on the "true image".

Nulls will appear in the final image at certain predetermined angles of incidence given by

$$\theta_n = \cos^{-1} \frac{(2n+1)\lambda}{2s}$$

where  $\lambda$  is the wavelength and  $s$  is the spacing between the deployer and the TS.

The range measurement allows the determination of the slant range  $R_n$  to a point on the null, and, therefore, the terrain profile can be computed for each line. The density of profiles can be increased by detecting other phases. The increasing distance between the deployer and the TS will decrease the spacing between nulls, which is directly related to profile accuracy.

Therefore the TSS provides the means to obtain or to update, by computer aided techniques, topographic maps at large scales not achievable from single space platforms, also in adverse weather and at any time, day or night.

Taking into account the significant international effort in the development of SAR's of increasing performance, the SAR-interferometer technique represents a potential improvement of active microwave application from space. For example a joint international program, such as the case of SIR-C and X-SAR (USA, FRG, Italy), can be envisaged to test, during a Shuttle demonstration flight, the achievable resolution and accuracy of a SAR-interferometer system.

#### A numerical simulation model

As previously shown, the relation between the TS attitude and position and the sensor viewing geometry must be accurately studied to limit the cost of the mission.

The problem of TS attitude and position control and determination is also present in many other proposed experiments and applications.

To this end, a simulation model has been developed which takes into account, contemporaneously, the TS orbital mechanics and attitude dynamics and the sensor observation geometry in order to identify the intersection of each line-of-sight or slant range on the Earth's ellipsoid (ref. 5). This model can be used to simulate and test the appropriate control laws of the tether length and of the TS attitude subsystem or to correct real images obtained during a remote sensing mission. A trade-off is therefore necessary between the design engineering constraints and the cost of a sophisticated preprocessing system.

The model developed to describe the TSS orbital dynamics is similar to the Skyhook approach (ref. 6). Moreover also the TS attitude dynamics is considered, taking into account the torques due to the tether tension and aerodynamic forces.

The sensor viewing geometry is simulated and the intersection of the line-of-sight with a digital elevation model, taking into account the atmospheric effects, is computed (ref. 7).

Different tests have been conducted to simulate the sensor observation from the TS, deployed by the Shuttle or a space station. The results have shown that, in-plane and out-of-plane oscillations do not affect significantly the geometric errors of the images taken during the short observation time interval. These oscillations and the longitudinal one can be damped by using an adequate tether control law.

As far as attitude is concerned, a deeper study is needed to identify the attitude measurement and control systems of the future multipurpose platform.

A meaningful test to check and improve the simulation model is the second demonstration mission where the TS will be deployed downwards to 100 Km.

To this end the authors have proposed using a lightweight metric camera to conduct a remote sensing experiment with the following objectives:

- to obtain high resolution stereoscopic coverage of several test sites for topographic and thematic applications;
- to integrate ground control points taken on the images with engineering and ancillary data for an improvement of the attitude and positional analysis of the TS during deployment, retrieval and station keeping;
- to focus the research community attention on the potentiality of the TS as a new remote sensing platform.

The present data rate necessarily implies the use of a film camera. This camera could provide different scales of coverage at different altitudes, depending on the required scale of the final map product. Tab. 2 shows the photographic scales obtainable during the proposed experiment with different focal lengths (F).

H Km	F cm	10	20	30
220		2,200,000	1,100,000	733,000
190		1,900,000	950,000	533,000
160		1,600,000	800,000	533,000
130		1,300,000	650,000	433,000

Table 2 Preliminary photographic scales from the TS metric camera.

The photographic scale is also connected to the elevation and position accuracy (ref. 8).

At this stage it is possible to give only a preliminary description of the metric camera characteristics, shown in tab. 3.

f/number	4
focal length	300 mm
film format size	11.5x11.5 cm
field of view	22°
ground resolution	10 m
ground footprint	50x50 Km
weight	15 Kg <sub>3</sub>
volume	10 dm <sup>3</sup>

Table 3 Preliminary characteristics of the metric camera.

The camera will utilize film supplied in a cassette of approximately 450 frames, with possibly a spacecraft forward motion compensation. Different time intervals between a photographic pair will be allowed, so providing various B/H ratios. An area of  $3.75 \times 10^5 \text{ Km}^2$ , equivalent to a strip of 7500 Km, will be covered with 35% overlap stereopairs and a B/H ratio of .25.

The metric camera accommodation in the TS is shown in fig. 10. The scientific package is allocated on the bottom, using an optical window at the end of a 18 cm diameter cylinder box, which has already been designed by Aeritalia (ref. 9). The upper part is connected to the P/L floor, equipped with special anti-vibration mounts.

Gaseous effluents eventually flowing near the optical window can affect the radiometric and geometric quality of the data and the external camera components through deposition and accumulation. The TSS gaseous effluents are of minor importance due to the thrusters distribution.

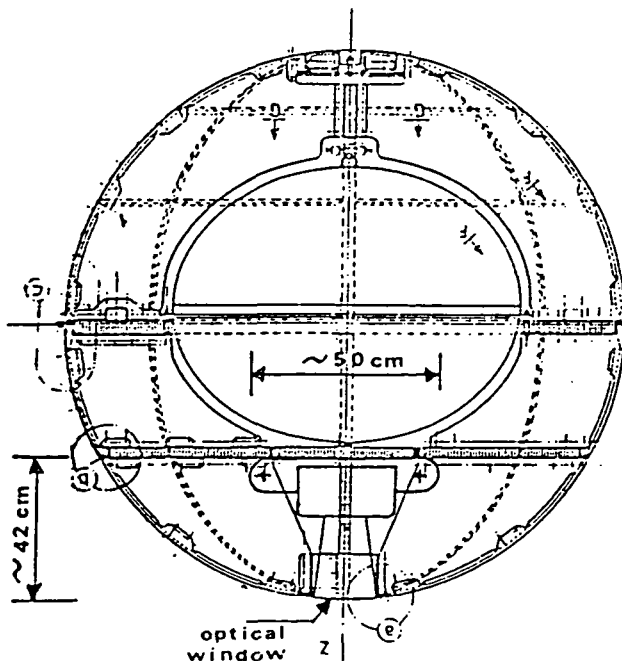


Fig. 10 The metric camera accommodation.

Determining the extent to which measurements may be degraded by spacecraft effluents and by atmosphere/satellite interactions requires a detailed study that can be integrated with other specific experiments.

By analyzing the stereoscopic photographs it will be possible to identify several Ground Control Points (GCP's), whose geographic coordinates and height are precisely known. The TS orbital and attitude simulation will be integrated with conventional photogrammetric techniques (ref. 10), and a more precise dynamics description will be carried out by using the GCP's and the satellite ancillary data.

The identification of GCP's requires, preferably, the observation of areas on which an appropriate cartography is available. Therefore the deployer orbit could be optimized by also taking into account the sun illumination condition. To this end different orbits are under study, as shown in the two examples of figs. 11-12. Both show the ground tracks relative to a TS 36 hours mission and to a solar elevation angle greater than  $30^\circ$ .

### Conclusions

The preliminary analysis, which has been carried out to verify the potentiality of the TS as a remote sensing platform, shows different advantages and peculiarities, particularly when high resolution and stereoscopic coverage are required.

In any case it is necessary to improve significantly the TS data rate and power (even using the tether as a power and communication line), and the control subsystems of the tether length and the TS attitude.

Also the technology of future space sensors requires taking into account the potentialities and new applications offered by the TS.

This new platform must be designed as a multipurpose satellite connected to the future space stations.

The simulation model, briefly described in this paper, requires a further substantial improvement which, on one hand, must be concentrated on the control laws, the tether behavior and the fluid oscillations in the containers, and, on the other hand, must utilize ad-hoc experiments to test the different model aspects.

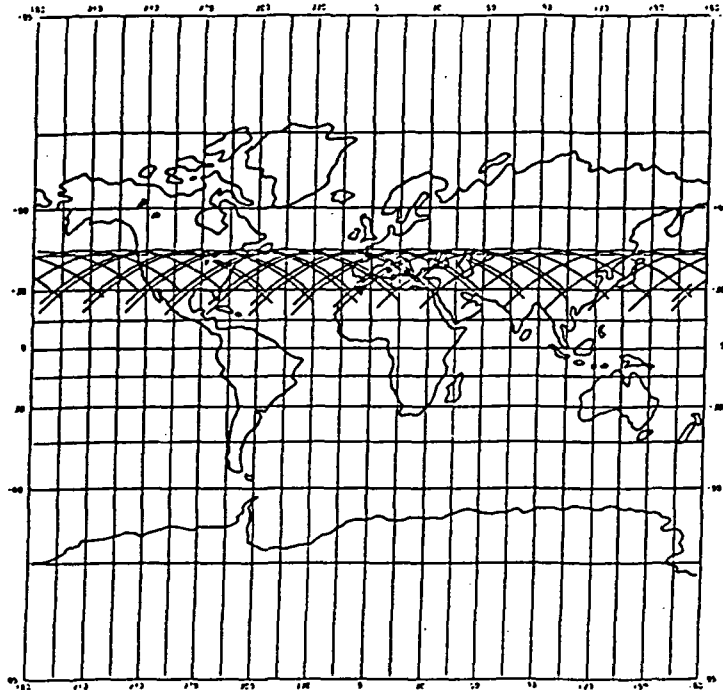


Fig. 11 Ground track of the drifting prograde orbit (deployer altitude Km 250, inclination  $47^\circ$ , nodal period 5363 s, repetition factor  $15+4/5$ ).

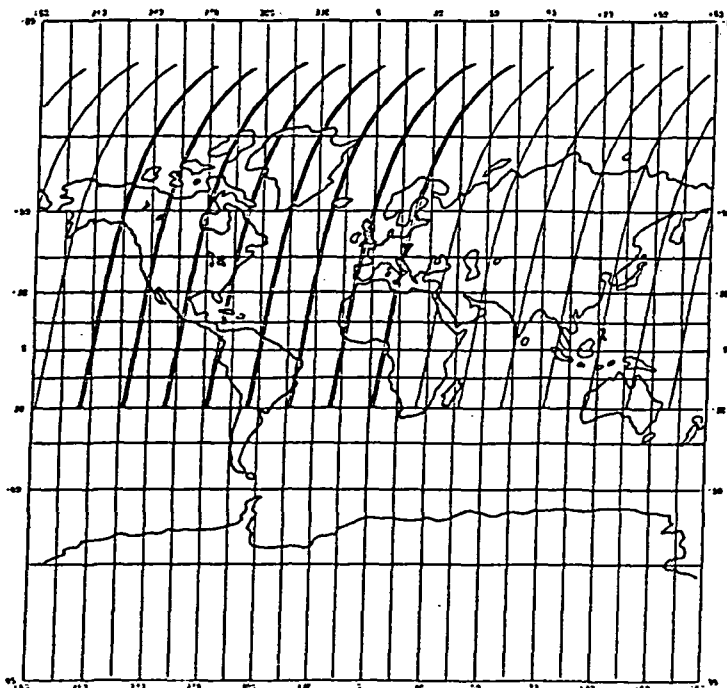


Fig. 12 Ground track of the drifting sunsynchronous orbit (deployer altitude Km 250, inclination  $96.5^\circ$ , nodal period 5378 s, repetition factor  $16+1/15$ ).

## References

1. Welch, R., 1980. Measurement from Linear Array Camera Images, Ph. Eng. and Rem. Sens., Vol. 46, No. 3, pp. 315-318.
2. Jet Propulsion Laboratory, 1979. Preliminary Stereosat Mission Description, NASA/JPL Report 720-33, May 30.
3. Harger, R.O., 1970. Synthetic Aperture Radar Systems, Theory and Design, Academic Press.
4. Ulaby, F.T., R.K. Moore, and A.K. Fung, 1982. Microwave Remote Sensing, Active and Passive, vol. II Radar Remote Sensing, Addison-Wesley.
5. Vetrella, S., and A. Moccia, 1985. Influenza della posizione e dell'assetto del Tethered Satellite System nell'osservazione stereoscopica dallo spazio, VIII Congr. AIDAA, 052-85.
6. Kalaghan, P.M., et al. 1978. Study of the Dynamics of a Tethered Satellite System (Skyhook), Smithsonian Inst. Astroph. Obser.
7. Moccia, A., S. Vetrella. An integrated approach to geometric precision processing of spaceborne high resolution sensors, accepted Int. Journal of Remote Sensing, Taylor & Francis.
8. Doyle, F.J., 1979. A Large Format Camera for Shuttle, Ph. Eng. and Rem. Sens., Vol. 45, No. 1, pp. 73-78.
9. Aeritalia, 1983. TSS, Satellite Module Baseline Design Review Presentation, Turin.
10. Ghosh, S.K., 1979. Analytical Photogrammetry, Pergamon Press.